Journal of Molecular Liquids 351 (2022) 118613

Contents lists available at ScienceDirect

Journal of Molecular Liquids

journal homepage: www.elsevier.com/locate/molliq

Hockey-Stick Polycatenars: Network formation and transition from one dimensional to three-dimensional liquid crystalline phases

Mohamed Alaasar [a,b,*], Silvio Poppe [a]

[a] Institute of Chemistry, Martin Luther University Halle-Wittenberg, Kurt Mothes Str. 2, D-06120 Halle (Saale), Germany
[b] Department of Chemistry, Faculty of Science, Cairo University, Giza, Egypt

ARTICLE INFO

Article history:
Received 12 December 2021
Revised 17 January 2022
Accepted 24 January 2022
Available online 29 January 2022

Keywords:
Polycatenar liquid crystals
Bent-core liquid crystals
Hockey-stick
Azobenzenes
Cubic phases
Photo switching

ABSTRACT

Photo switchable liquid crystalline (LC) materials are of great interest for optical and photonic applications. Herein we report the design, synthesis, and molecular self-assembly of the first examples of photosensitive hockey-stick (HS) polycatenars. Therefore, two new series of HSLCs derived from 4-cyanoresorcinol bent-core unit connected to a short azobenzene-based side arm with one variable alkoxy chain and a long ester-based wing terminated with two alkoxy chains at 3 and 5 positions of the terminal benzene ring are reported. They differ from each other in the length of the terminal chains connected to the long arm. The LC self-assembly of these HSLCs was investigated by polarized optical microscopy (POM), differential scanning calorimetry (DSC), X-ray diffraction (XRD) and electro optical investigations. Depending on length of terminal chains a transition from one dimensional (1D) tilted and non-tilted smectic phases to three dimensional (3D) achiral bicontinuous cubic phases with $Ia\bar{3}d$ symmetry ($Cub_{bi}/Ia\bar{3}d$) upon chain elongation is observed. Moreover, achiral isotropic liquid networks were observed for medium and long chain homologues. Most of mesophases are room temperature LCs phases with wide ranges as observed in the cooling cycles, where once they are formed on heating, no sign of crystallization is detected down to ambient temperature. Finally, UV light irradiation results in fast and reversible photoinduced transformation between different types of LCs phases as well as between LC phase and isotropic liquid.

1. Introduction

Designing materials with potential nano-technological applications is of great interest. Liquid crystals (LCs) represent one class of such materials which are widely applied nowadays in electronic and optoelectronic devices [1,2]. LCs have not only been applied in liquid crystals displays (LCDs) but also as organic semiconductors in organic field effect transistors (OFETs) [3], organic light emitting diodes (OLEDs) [4], and organic photovoltaic cells (OPV) [5]. Besides conventional rod-like LCs, bent-core liquid (BCLCs) represent an interesting class of nonconventional LCs, which exhibit unique and fascinating mesophases ranging from polar smectic to non-polar smectic phases known to be formed by rodlike LCs [6–11]. More interesting, BCLCs can form spontaneously mirror symmetry broken mesophases such as the helical nanofilament phase (B4 phase) [12,13] and dark conglomerate phases (DC phases) [14,15], though the molecules themselves are achiral. BCLCs can also display cybotactic and paraelectric nematic phases [16,17] in addition to their potential to form biaxial nematics.[18–22]. Due to their reversible *trans–cis* photoisomerization upon light irradiation azobenzene-based BCLCs have attracted the attention of many researchers [11,23–29]. The presence of the azobenzene unit in the molecular structure provides an efficient way to photocontrol the molecular structure and to modulate the physical properties toward applications [30]. Therefore, azobenzene based LCs have been applied in optoelectronic sensing devices [31] and organic light-driven actuators [32–34]. Recently, we have reported different classes of azobenzene containing BCLCs derived from 4-substituted resorcinol core unit that exhibit mirror-symmetry breaking in helical nano-crystallite phases (HNC) [11,15] as well as in fluid smectic C phases depending on the type of the substituent used [35–38]. One of the most promising central core units is 4-cyanoresorcinol, which is known to induce LC mesophases at the border line between rod-like and bent-core molecules [36–43]. A breakthrough came with the discovery of mirror-symmetry breaking in the liquid networks known as $Iso_1^{[*]}$ formed by polycatenars [44,45]. Polycatenars represent another class of nonconventional LCs consisting of a long aromatic rod-like core

* Corresponding author at: Institute of Chemistry, Martin Luther University Halle-Wittenberg, Kurt Mothes Str. 2, D-06120 Halle (Saale), Germany.
E-mail address: mohamed.alaasar@chemie.uni-halle.de (M. Alaasar).

https://doi.org/10.1016/j.molliq.2022.118613
0167-7322/

decorated with multiterminal flexible chains [46]. Due to nanosegregation of the aromatic rigid core and the terminal flexible chains, polycatenars can display different types of LCs mesophases including nematic, smectic, bicontinuous cubic (Cub_{bi}), micellar cubic and columnar phases depending on the number of the terminal chains. Cub_{bi} phases are three dimensional LCs phases, which represent an intermediate state between the one dimensional (1D) lamellar and the two dimensional (2D) columnar mesophases and are very interesting for a wide range of applications e.g. as 3D conducting or photonic materials [47,48], and for optical bandgap materials [49–51]. These 3D phases with cubic symmetry are rarely observed in bent-core molecules [52–55], while they are known to be formed by polycatenars having terminal chains nonsymmetrically distributed at both ends of the long aromatic core [44,45,56–59]. There are two types of Cub_{bi} formed by such polycatenars, the first one is achiral Cub_{bi} with $Ia\bar{3}d$ symmetry (Cub_{bi}/$Ia\bar{3}d$) [60], and the second type is chiral Cub_{bi} with I23 symmetry ($Cub_{bi}^{[*]}$/$I23$) [61]. The two different types are characterized by their high viscosity and can be distinguished by XRD investigations [60,61]. Under POM with crossed polarizers both of them appear totally isotropic, while under slightly uncrossed polarizers dark and bright areas could be only observed in the case of the chiral $Cub_{bi}^{[*]}$/$I23$. These domains invert their signs by inverting the direction of rotation of the analyzers, confirming the chirality of this $Cub_{bi}^{[*]}$/$I23$ phase. The $Iso_{I}^{[*]}$ phase was found to be formed beside either the chiral $Cub_{bi}^{[*]}$/$I23$ or the achiral Cub_{bi}/$Ia\bar{3}d$ phases in most cases [44,45,56,57,58,59,62]. However, we have also reported recently the first example of an $Iso_{I}^{[*]}$ phase occurring beside a Smectic A (SmA) phase exhibited by azobenzene-based tricatenars [63]. The latter was also able to form the achiral version of the 3D Cub_{bi} phases i.e. Cub_{bi}/$Ia\bar{3}d$ beside SmA and other different types of smectic phases depending on the length of the terminal alkyl chain [64]. Therefore, the question arose if the LC phases of polycatenars still show chiral mesophases if a bend is induced in its molecular structure by using 4-cyanoresorcinol as central bent unit (see scheme 1), which known to have low bend angle < 120° [36,37,38,39,40,41,42,43]. Moreover, would this molecular structure exhibit banana-mesophases or other LCs phases that are displayed by HS molecules?

To answer these two questions, herein we report the synthesis and investigation of the liquid crystal self-assembly of a new family of polycatenars in the form of hockey-stick (HS) molecules derived from 4-cyanoresorcinol connected to two side arms, where one arm is much longer than the other (**A6/*n*** and **A10/*n***, Scheme 2). HSLCs represent materials that could display mesophases at the cross over between BCLCs and rod-like molecules which could also lead to new mesophases [65–79]. The new HS molecules represent tricatenar systems having two terminal alkyl chains attached to the long side arm at positions 3 and 5 on the terminal benzene ring and one alkyl chain attached to the azobenzene-based short side arm. Therefore, two different series of these HS molecules **A6/*n*** and **A10/*n*** (see Scheme 2 and Fig. 1) were designed and synthesized, where in the first series the double chain on the long side arm are kept fixed with 6 carbon atoms in each chain i.e. hexyloxy chains and in the second series they are replaced by decyloxy chains. In both series of compounds, the number of carbon atoms in terminal chain attached to the azobenzene-based wing i.e. the short arm was varied between n = 6 → 16. To the best of our knowledge **A6/*n*** and **A10/*n*** compounds are the first examples of photosensitive hockey-stick polycatenars reported up to date. The mesophase behaviour of these new HS has been investigated by polarizing optical microscopy (POM), differential scanning calorimetry (DSC), X-ray diffraction (XRD) and electro optical measurements.

2. Experimental

2.1. Synthesis

The synthesis of the target HS polycatenars **A6/*n*** and **A10/*n*** was performed as shown in Scheme 2. The azobenzene containing benzoic acids derivatives (**1/*n***) were prepared as described before [35], while the synthetic procedures for the benzoic acid derivatives terminated with double chains are recently reported elsewhere [80]. All final HS molecules were synthesized by acylation reaction of the hydroxy compounds **3/*n*** with one equivalent of the acid chloride derived from azobenzene-based benzoic acid derivatives **4/*n***. The acylation reactions were carried out in presence of triethylamine as a base and a catalytic amount of pyridine. The crude final materials were purified firstly by column chromatography using dichloromethane as an eluent followed by recrystallization from ethanol/chloroform (1:1) mixture to yield the target HS polycatenars. The synthesis details of all intermediates as well as the final materials and the analytical data are reported in the Electronic Supporting Information (ESI). All compounds are thermally stable as proved by the reproducibility of DSC thermograms in repeated heating and cooling cycles.

2.2. Methods

The thermal behaviour of all synthesized compounds was studied by polarizing optical microscopy (POM) and differential scanning calorimetry (DSC). For polarizing microscopy a Mettler FP-82 HT hot stage and control unit in conjunction with a Nikon

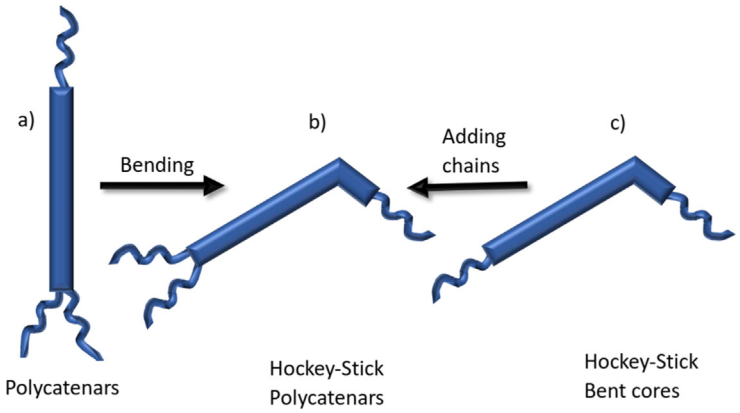

Scheme 1. Molecular design principle of the new hockey-stick polycatenars.

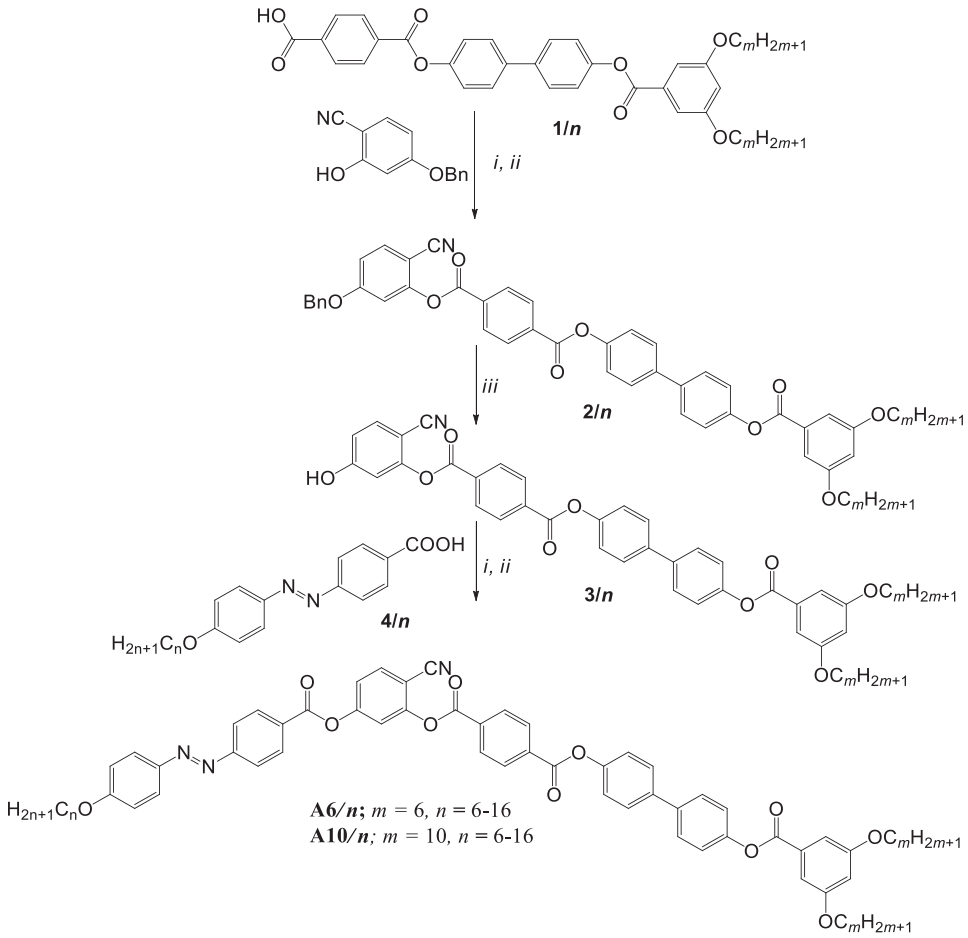

Scheme 2. Synthesis of the target HS polycatenars **A6/*n*** and **A10/*n***. Reagents and conditions: *i*) DMF, $SOCl_2$, reflux 1 hr.; *ii*) dry CH_2Cl_2, dry TEA, dry pyridine, reflux for 6 hr; *iii*) H_2, Pd/C-10%, dry THF, stirring 24 hr.

Optiphot-2 polarizing microscope was used. DSC-thermograms were recorded on a Perkin-Elmer DSC-7 with heating and cooling rates of 10 K min^{-1}. Electro-optical switching characteristics were examined in 6 μm polyimide coated ITO cells (EHC Japan) using the triangular-wave method [81]. XRD patterns were recorded with a 2D detector (Vantec-500, Bruker). Ni filtered and pin hole collimated CuK_α radiation was used. The exposure time was 15 min and the sample to detector distance was 27.4 and 9.5 cm for small angle and wide angle scattering experiments, respectively. Alignment was attempted by slow cooling (rate: 1 K min^{-1} to 0.1 K min^{-1}) of a small droplet on a glass plate.

3. Results and discussion

3.1. Hockey-stick polycatenars *A6/n*

Compounds **A6/*n*** having two hexyloxy chains attached at position 3 and 5 in the terminal benzene ring of the long side arm of the HS molecules form two different types of enantiotropic mesophases (see Table 1 and Fig. 1).

The shortest compound **A6/6** with n = 6 forms tilted and non-tilted smectic phases. On cooling **A6/6** from the isotropic liquid a transition to a highly birefringent phase with a fan shaped texture associated with dark areas are observed at $T \sim 142$ °C as typically observed for non-tilted smectic A (SmA) phases. Therefore, the higher temperature LC phase of **A6/6** is assigned as SmA phase. On further cooling and at $T \sim 99$ °C, a weak birefringence is induced in the dark areas observed in Fig. 2a, while the fan shaped textures are not altered and the directions of the dark extinctions observed in Fig. 2a and b are the same, confirming a transition from SmA phase to the rarely observed anticlinic tilted SmC phase i.e. SmC_a [79], which remains without crystallization till room temperature. The crystallization is only observed on heating cycle and the same phase sequence is observed on heating and cooling scans confirming the enantiotropic nature of these LCs phases. The SmC_a-SmA phase transition could be also detected by DSC investigations (see Table 1 **and** Fig. 3**a**). On chain elongation the SmC_a phase is removed for all longer homologues with $n \geq 8$, where SmA is the only observed mesophase (see Table 1 and Fig. 1).

For all medium chain compounds with n = 8–12, the SmA remains till room temperature on cooling without crystallization, which is only observed for longer homologues with $n \geq 14$. Another interesting feature of compounds **A6/*n*** is the observation of a broad peak in the DSC curves in the isotropic liquid range for compounds **A6/12** - **A6/16** (see Fig. 3**b**). This broad feature is observed on cooling cycle only for **A6/12** and on both heating and cooling cycles in case of **A6/14** and **A6/16**. By rotating one of the analyzers from the crossed position in the temperature range of this isotropic liquid phase for any of **A6/12** - **A6/16** compounds no dark and bright domains could be observed indicating that this isotropic liquid is not chiral as reported before for related linear tricatenars.[63,64] Therefore, this achiral isotropic liquid phase is designated as Iso_1 without asterisk. As can be seen from Table 1, the enthalpy value of LC-Iso transition either on heating or cooling is relatively large, indicating a significant packing density of the

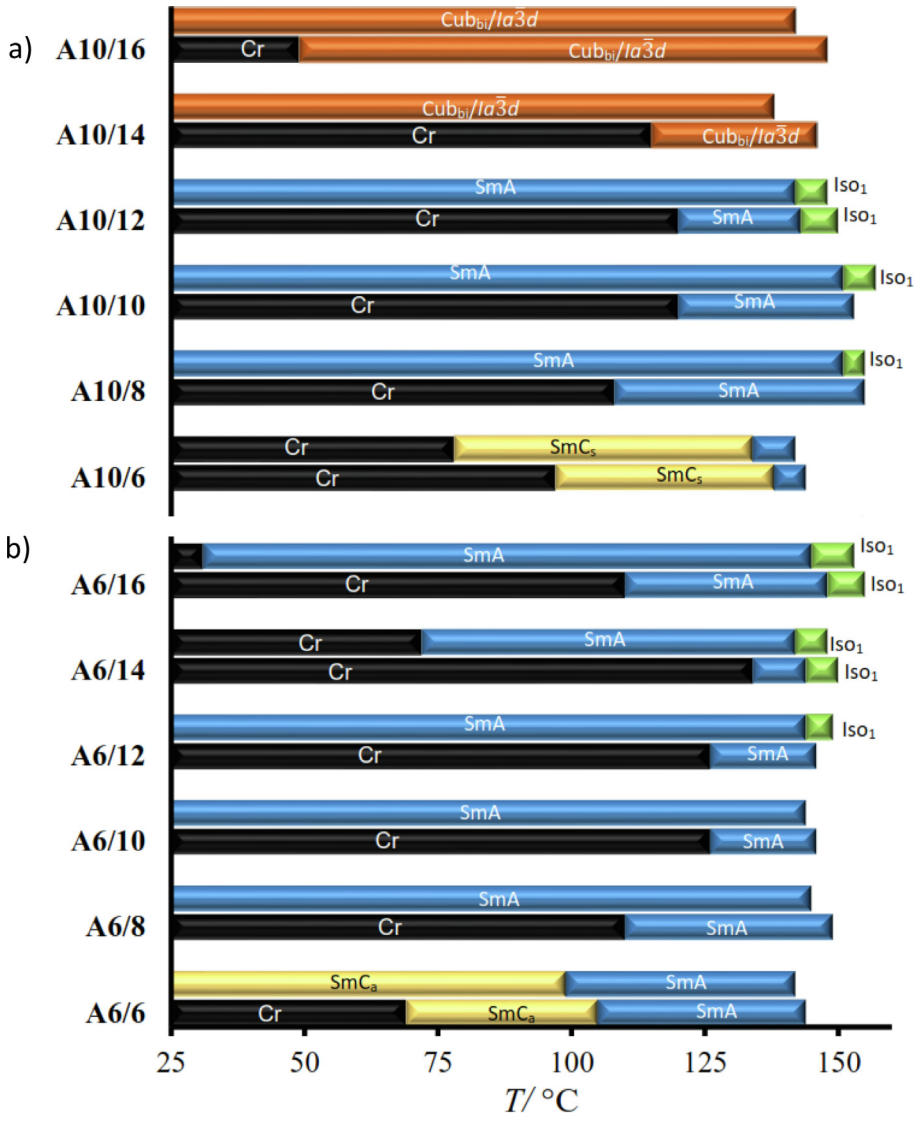

Fig. 1. Phase behaviour of the investigated new polycatenars on heating (lower bars) and on cooling (upper bars) for: a) series **A10/*n*** and b) series **A6/*n***. For abbreviations see Table 1.

long aromatic cores, which simultaneously stabilizes the smectic phases and thus lead only to the formation of SmA phases in most cases.

To confirm the type of the smectic phases formed by **A6/*n*** compounds, we performed X-ray diffraction (XRD) investigations for some selected examples. In the higher temperature smectic phase of compound **A6/6** at 120 °C a diffuse scattering is observed in the wide-angle region, while one sharp Bragg reflection in the small angle region (see Fig. 4**a**) corresponding to d = 5.63 nm is observed. This indicates that this phase represents a smectic phase without in-plane positional order. The maximum of the diffuse scattering in the wide-angle region is perpendicular to the small angle reflections, which confirms an on average non-tilted organization of the molecules in the layers i.e. a SmA phase in agreement with the observed optical texture in this LC phase. The experimental d-value is larger than the molecular length of a single molecule (L_{mol} = 4.44-nm), determined with Materials Studio for a V-shaped conformation with bending angle of 120° and all-trans stretched alkyl chains (see Fig. 5). This indicates an antiparallel side-by-side packing of the molecules in layers with partial interdigitation of the alkyl chains and aromatic cores (Fig. 5a).

In the temperature range of the other smectic phase and at T = 60 °C, the d-value decreases only slightly to be d = 5.55 nm (Fig. 4**b**), in line with a tilted organization of the molecules and indicated by the weak birefringence texture in this LC phase (Fig. 2b). Based on the small difference between layer spacing in SmA and SmC phases, it is likely that the SmA phase is of the de Vries type [82,83]. It should be noted that XRD measurments cannot precisely differentiate between the synclinic and anticlinic SmC phases [79,84]. However, based on the XRD results and the textural observations of **A6/6** at T = 60 °C, this phase is assigned as a anticlinic tilted smectic C phase i.e. SmC$_a$.

3.2. Hockey-stick polycatenars A10/n

Replacing the two terminal hexyloxy chains in compounds **A6/*n*** with two longer decyloxy chains leads to the formation of series **A10/*n***. The phase sequence and types of mesophases formed by **A10/*n*** derivatives are given in Table 1 and represented graphically in Fig. 1**a**. As can be seen from Table 1 and Fig. 1a, the shortest homologue **A10/6** exhibit SmA and SmC phases as observed for the related analogue **A6/6**. However, the SmA phase range of

Table 1
Phase transition temperatures (T/°C), mesophase types, and transition enthalpies [ΔH/kJ·mol^{-1}] of compounds **A6/*n*** and **A10/*n***.[a].

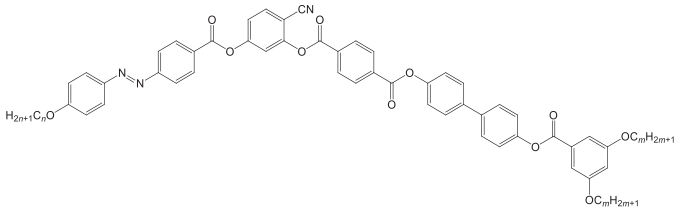

Cpd.	*m*	*n*	*Transition Temp.*
A6/6	6	6	**H:** Cr 69 [9.5] SmC_s 105 [0.6] SmA 144 [2.4] Iso **C:** Iso 142 [2.2] SmA 99 [0.8] SmC_s < 20 Cr
A6/8	6	8	**H:** Cr 110 [32.7] SmA 149 [3.2] Iso **C:** Iso 145 [3.1] SmA 96 < 20 Cr
A6/10	6	10	**H:** Cr 126 [36.4] SmA 146 [2.6] Iso **C:** Iso 144 [2.6] SmA < 20 Cr
A6/12	6	12	**H:** Cr 126 [38.3] SmA 146 [3.7] Iso **C:** Iso 149 [0.1] Iso_1 144 [2.4] SmA < 20 Cr
A6/14	6	14	**H:** Cr 134 [52.0] SmA 144 [1.2] Iso_1 150 [1.0] Iso **C:** Iso 148 [2.1] Iso_1 142 [1.2] SmA 72 [16.0] Cr
A6/16	6	16	**H:** Cr 110 [25.6] SmA 148 [0.8] Iso_1 155 [1.3] Iso **C:** Iso 153 [0.9] Iso_1 145 [0.8] SmA 31 [5.6] Cr
A10/6	10	6	**H:** Cr 97 [25.6] SmC_a 138 [0.5] SmA 144 [4.8] Iso **C:** Iso 142 [4.6] SmA 134 [0.6] SmC_a 78 [24.8] Cr
A10/8	10	8	**H:** Cr 108 [27.0] SmA 155 [2.3] Iso **C:** Iso 155 [2.4] Iso_1 151 [1.6] SmA < 20 Cr
A10/10	10	10	**H:** Cr 120 [38.8] SmA 153 [2.0] Iso **C:** Iso 157 [7.3] Iso_1 151 [1.8] SmA < 20 Cr
A10/12	10	12	**H:** Cr 120 [29.8] SmA 143 [0.8] Iso_1 150 [2.0] Iso **C:** Iso 148 [3.0] Iso_1 142 [0.8] SmA < 20 Cr
A10/14	10	14	**H:** Cr 115 [39.4] $Cub_{bi}/Ia\bar{3}d$ 146 [1.3] Iso **C:** Iso 138 [0.5] $Cub_{bi}/Ia\bar{3}d$ < 20 Cr
A10/16	10	16	**H:** Cr 49 [43.8] $Cub_{bi}/Ia\bar{3}d$ 148 [2.2] Iso **C:** Iso 142 [1.7] $Cub_{bi}/Ia\bar{3}d$ < 20 Cr

Notes: [a]Transition temperatures and enthalpy values were taken from the second DSC heating scans (**H**) and cooling scans (**C**) with 10 K min^{-1}; abbreviations: Cr = crystalline solid; SmC_s = synclinic smectic C phase; SmC_a = anticlinic smectic C phase; SmA = orthogonal non-tilted smectic A phase; Cub_{bi}/Iad = achiral cubic phase with $Ia\bar{3}d$ lattice; Iso_1 = achiral isotropic liquid; Iso = isotropic liquid.

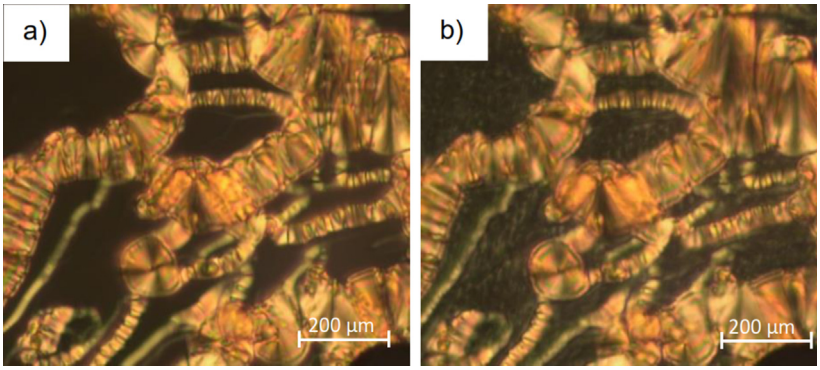

Fig. 2. Optical micrographs observed for compound **A6/6** in a homeotropic cell (ordinary non-treated microscopy slides) on cooling in: a) in the SmA phase at T = 130 °C and b) in the SmC_a phase at T = 60 °C.

A10/6 is narrower as would be expected by chain elongation and the SmC phase is crystallized on cooling and not a room temperature LC phase as that exhibited by **A6/6**.

More interesting, the SmC phase of **A10/6** is synclinicly tilted and not anticlinicly tilted as that of **A6/6**. The synclinic tilt is confirmed by the high birefringence of the SmC exhibited by **A10/6** compared to the weak birefringence of that of **A6/6** (compare Fig. 6**a** and the homeotropic regions in Fig. 2b). Moreover, a schlieren texture with four brush disclinations could be observed, which also confirms the presence of a synclinic SmC i.e. SmC_s mesophase [79]. To further confirm the SmC_s-SmA transition, the optical textures were recorded in a planar 6 µm ITO cell, where the fan textures observed in the SmA phase became broken in the SmC_s phase accompanied by increasing of birefringence (Fig. 6c, d).

To test if the smectic phases formed by **A6/6** and **A10/6** are polar or not, electro-optical experiments were performed using a triangular wave voltage for these two compounds. For both materials no current peak could be observed neither in the SmA, nor in the SmC_s phases of these two materials up to a voltage of 200 V_{pp} in a 6 µm ITO cell, indicating the non-switching behaviour and the non-polar nature of these two phases. The loss of polar order in these smectic phases indicate that they are different from those

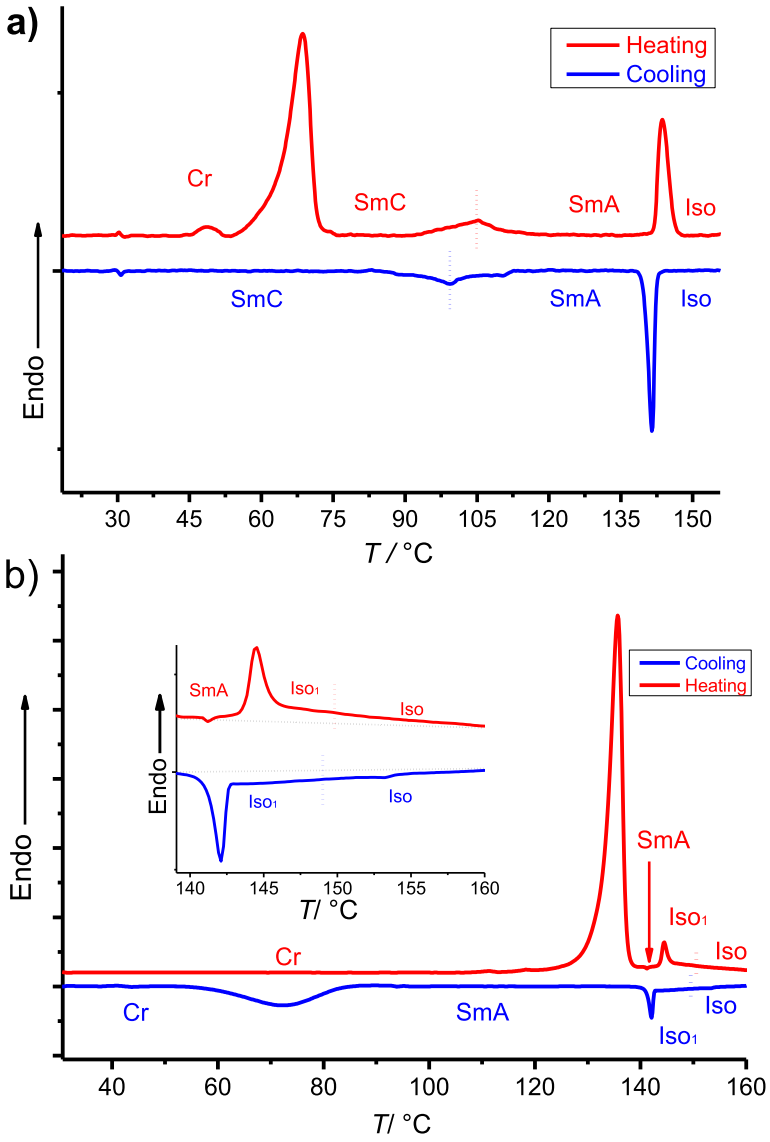

Fig. 3. DSC thermograms obtained for: a) compound **A6/6** and b) **A6/14**; with 10 K min^{-1} heating and cooling rates. The inset in b) represents an enlarged range (138 °C-160 °C) showing the Iso_1-Iso broad transition peaks on heating and cooling cycles of **A6/14**.

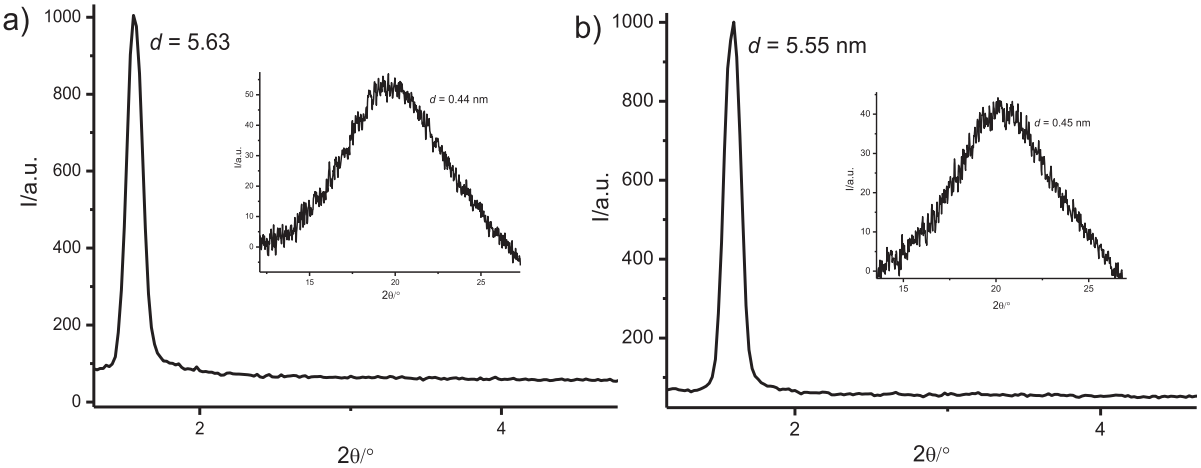

Fig. 4. Small X-ray diffraction (SAXD) patterns of **A6/6** at: a) T = 120 °C in the SmA phase and b) T = 60 °C in the SmC_a phase. The insets show the wide-diffraction patterns (WAXD).

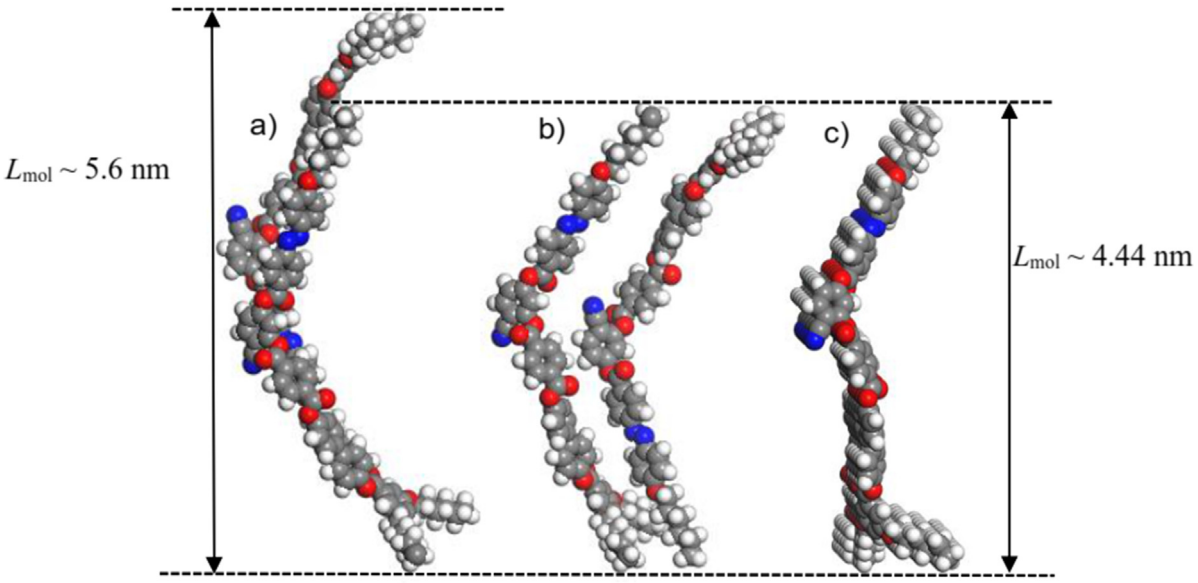

Fig. 5. Space-filling models of **A6/6** showing the distinct modes of self-assembly in the SmA layers (one layer is represented): a) intercalated bilayer structure with antiparallel (up-down symmetric) arrangement of the molecules, b) antiparallel arrangement of the molecules with complete segregation of aromatic cores and aliphatic chains and c) parallel organization of the molecules with complete segregation of chains and cores.

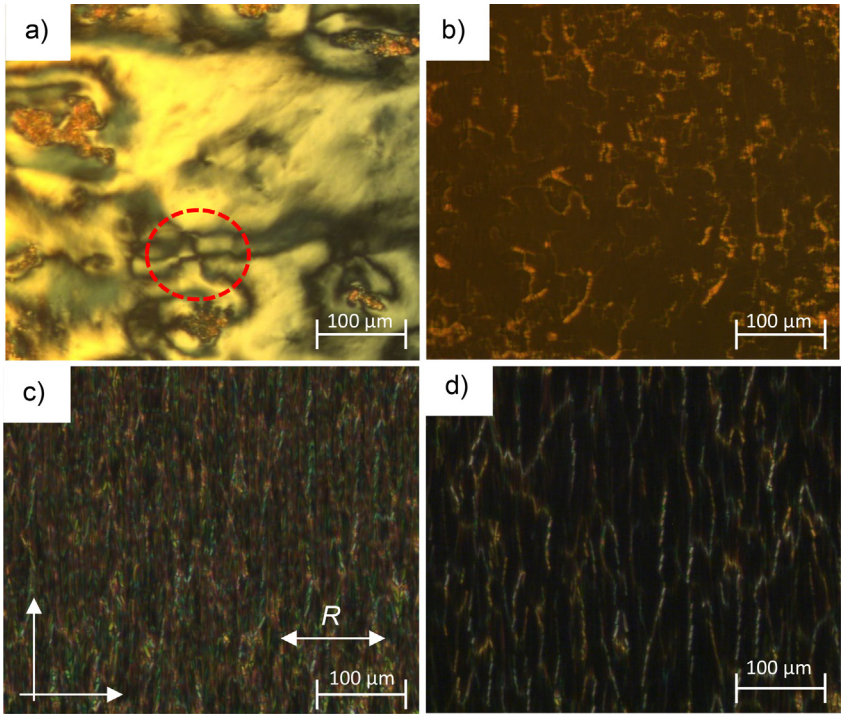

Fig. 6. Optical micrographs observed for compound **A10/6** in: a), b) a homeotropic cell (ordinary non-treated microscopy slides) in the SmC_s phase at T = 100 °C a); in the SmA phase at T = 110 °C b); The red dashed circle in a) indicates the four brush defects, which confirm the presence of SmC_s phase; c), d) in a planar 6 µm ITO cell c) the SmC_s phase at T = 100 °C and d) the SmA phase at T = 110 °C. The directions of polarizers and analyzer and the rubbing direction (R) are indicated in c).

usually observed in BCLCs, which might be attributed to the distorted packing of the molecules as described above giving rise to a significant distortion for the directed packing of the bent directions of the cores (see Fig. 5). A polar order could be expected if a uniform bend-direction with preferred packing of the bent-core molecules with parallel organization could be achieved (Fig. 5c), which is not the case in our molecules. This behaviour is like other previously reported HS molecules, which also exhibit non-polar smectic phases in most cases.[65–79]

On chain elongation the SmC_s phase is removed and the SmA phases are formed beside the liquid networks i.e. Iso_1 phases for all medium chain derivatives with n = 10–12 (see Fig. 1b). The Iso_1 phase is formed as a metastable phase for **A10/8** and as enantiotropic one for **A10/10** and **A10/12**. Moreover, the SmA phases of

these medium chain compounds are stable down to room temperature as once they formed on heating, they do not show any sign of crystallization on cooling cycles (Fig. 1a). On further chain elongation and with $n \geq 14$ the SmA phase is replaced by another highly viscous phase, which is characterized by its isotropic appearance under crossed polarizers as observed in POM investigations. This indicates the formation of a cubic liquid crystalline phase which is not exhibited by any other homologues of **A6/*n*** or **A10/*n*** derivatives. On rotation one of the analyzers from the crossed position with a small angle either in clockwise or anti clockwise direction no dark and bright domains could be seen, indicating that this phase is of achiral nature. Also, for this LC phase there is ~ 6 K supercooling of the Iso–LC transition compared to the LC–Iso transition temperature on heating (see Table 1 and Fig. 1b) which is a typical feature of cubic LC phases.

These observations are all typically observed for the achiral bicontinuous cubic phase with $Ia\bar{3}d$ space group ($Cub_{bi}/Ia\bar{3}d$) [45,59,64]. This cubic phase is formed for both **A10/14** and **A10/16** as an enantiotropic phase with very wide temperature range on heating for the longest homologue **A10/16**, which became even room temperature stable phase for both materials on cooling from the isotropic liquid phase (see DSC traces of **A10/14**, Fig. 7**b**). Compound **A10/14** was further investigated with XRD investigation to confirm the type of the Cub_{bi} phase (Fig. 8). The two most intense peaks in the SAX pattern (Fig. 8) can be indexed to the (211) and (220) reflections, confirming a Cub_{bi} phase with $Ia\bar{3}d$ lattice with a calculated lattice parameters a_{cub} of 13.3 nm, which is also in the expected range.

3.3. Photosensitivity

The HS polycatenars **A6/*n*** and **A10/*n*** were designed to be photo switchable by incorporation of the photosensitive azo unit in their molecular structures. Therefore, the geometry of the azo unit could be changed by UV/Vis light irradiation due to *trans–cis* photoisomerization, which leads to breaking of the supramolecular order, and thus to phase modulation. Recently, interesting photoswitching properties were reported for azobenzene-based polycatenars [85–88] as well as for azobenzene-based BCLCs [23–29,35,36]. The new HS polycatenars reported herein except **A10/14** and

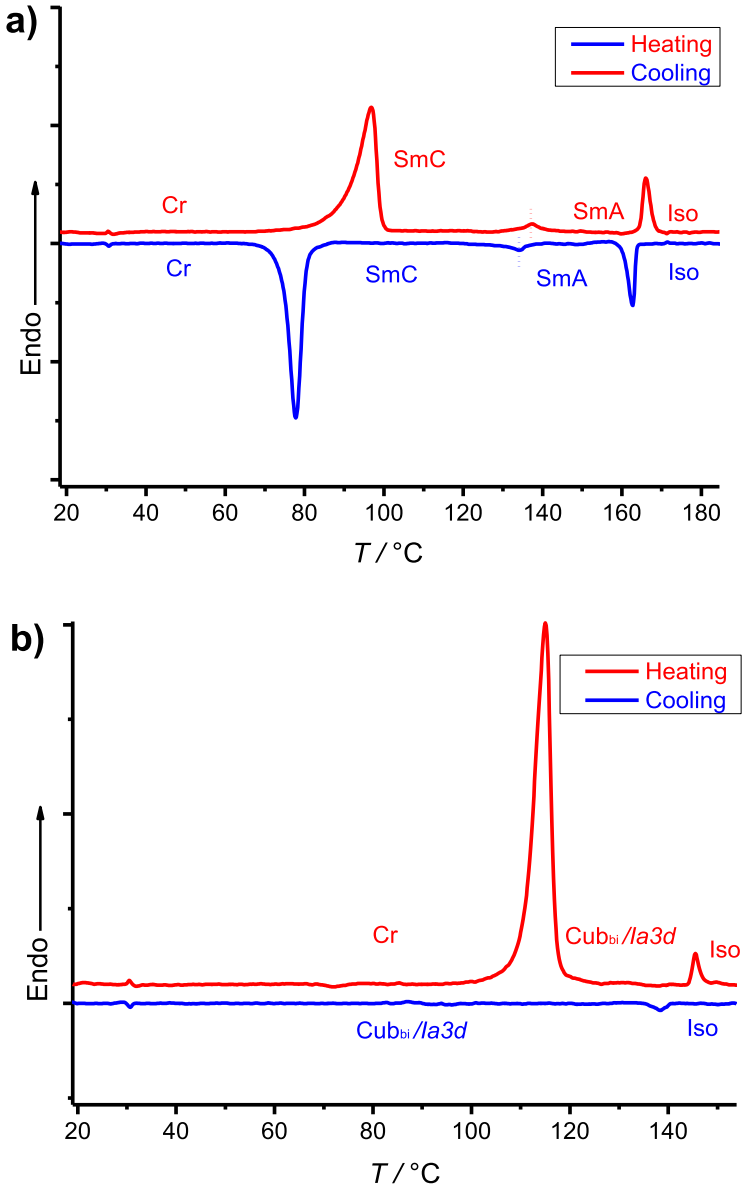

Fig. 7. DSC thermograms obtained for: a) compound **A10/6** and b) **A10/14**; with 10 K min^{-1} heating and cooling rates.

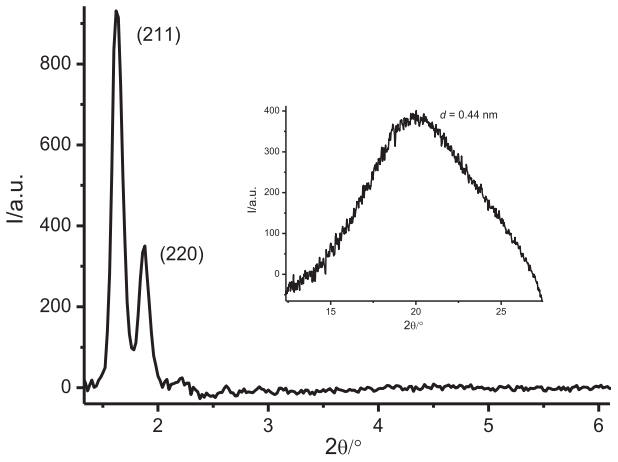

Fig. 8. Small X-ray diffraction (SAXD) patterns of **A10/14** at T = 110 °C in the Cub_{bi}/*Ia3d* phase. The inset shows the wide-diffraction patterns (WAXD) at the same temperature.

A10/16 undergo a fast and reversible isothermal phase transition upon illumination with UV laser pointer (405 nm, 5 mW/mm^2). As a representative example, Fig. 9 shows the results observed for compound **A10/6** under POM. Fig. 9**a** shows the birefringent texture of the SmC_s phase at ~ T = 100 °C prior to light irradiation, which upon light illumination changes to the oily streak characteristic texture of the SmA phase, coexisting with homogenously aligned regions which appear black under crossed polarizers (Fig. 9b). On switching off the light source, the SmA phase transforms back in<3 s to the SmC_s phase. Similar observation was also observed in the SmA phase, where a transformation to the isotropic liquid was achieved upon light irradiation of the SmA phase within < 3 s (Fig. 9b, c), which also relaxes back to the SmA texture very quickly on removing the light source. These observations indicate a fast and an efficient photoinduced phase transition between different types of LCs phases as well as between SmA and isotropic liquid i.e. isothermal photoinduced phase transitions as a result of *trans–cis* photoisomerization of the azobenzene units.

3.4. Comparison with related linear polycatenars

By comparing the phase behaviour of the newly reported HS polycatenars reported herein **A6/*n*** and **A10/*n*** with the recently reported rod-like polycatenars **B*n*** (Scheme 3) [63,64] having also an extended aromatic core but missing the central 4-cyanoresorcinol core which induces bending of the molecule we can reach the following conclusions.

Depending on the terminal chain length in case of linear polycatenars **B*n*** a rich variety of LCs phases were observed, including hexatic phases ($HexI_s$, HexB), non-tilted smectic A (SmA), synclinic and anticlinic tilted smectic C phases (SmC_s, SmC_a), a long pitch heliconical SmC phase as well as Cub_{bi}/$Ia\bar{3}d$ in addition to the chiral $Iso_1^{[*]}$ and the achiral Iso_1 isotropic liquid mesophases. The formation of the rare anticlinic SmC_a phases is a characteristic feature of HS molecules, which notably formed by the linear tricatenars **B*n*** and only for the new HS molecule **A10/6**. This means that **B*n*** compounds combine the properties of conventional HS materials and those of nonsymmetric polycatenars. On the other hand, for the HS **A6/*n*** and **A10/*n*** such rich mesomorphism was not observed and no chiral mesophases were formed as those exhibited by **B*n*** materials. Obviously, the introduction of the central bent-core unit in the structure of the rod-like polycatenars **B*n*** retain some mesophases formed by the nonsymmetric polycatenars such as the achiral Iso_1 and Cub_{bi}/$Ia\bar{3}d$ phases but at the same time suppress the formation of any chiral phases and any of the known banana mesophases as one would expect. This might be explained by removing the polar order in **A6/*n*** and **A10/*n*** HS polycatenars because of the antiparallel organization of the molecules with partial interdigitation of the alkyl chains in the aliphatic layers (Fig. 5a). Another possible explanation could be the low bending angle provided by the 4-cyanoresorcinol core unit, resulting in the formation of LCs phases at the border line between conventional rod-like molecules

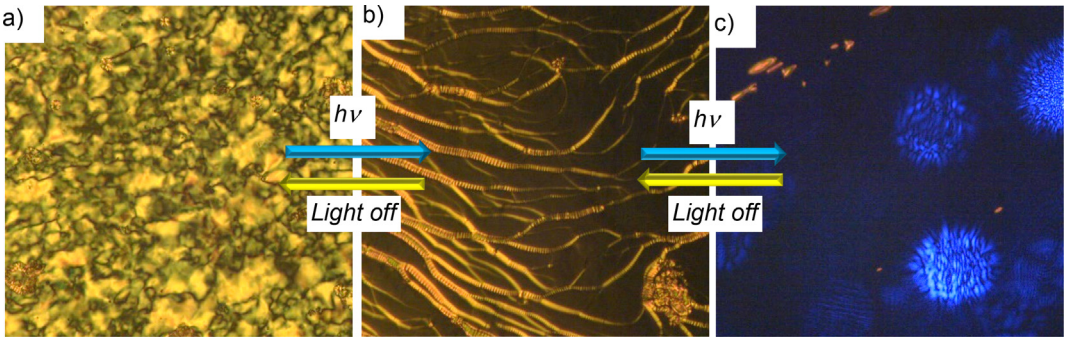

Fig. 9. Optical textures observed on heating for compound **A10/6** under crossed polarizers: a) in the SmC_s phase at T = 100 °C before irradiation with UV light and b) after irradiation with UV light showing the transformation from the SmC_s phase to the SmA phase and c) in the isotropic liquid phase after light irradiation of the SmA phase at 140 °C. The blue dots in c) are due to UV light.

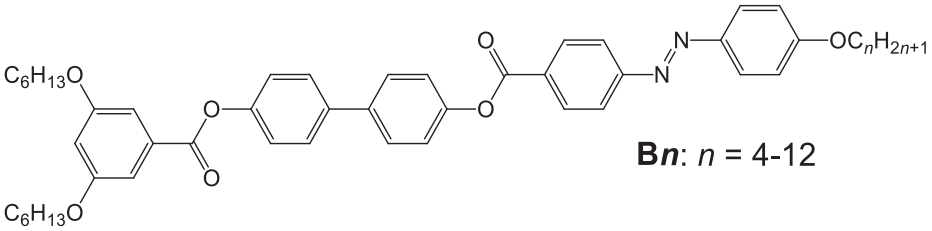

Scheme 3. Previously reported rod-like polycatenars **B*n*** [63,64].

and BCLCs. This needs further investigation and synthesis of related materials using different types of central core units to reach the right core unit able to combine the LCs mesophases of both BCLCs and polycatenars. However, notably the SmA phases exhibited by all **A6/*n*** homologues and the short and medium chain homologues of **A10/*n*** series represent room temperature LC phases as observed on cooling cycles for all materials (Fig. 1), whereas no ambient temperature LCs phases were formed by any of **B*n*** compounds. Moreover, the $Cub_{bi}/Ia\bar{3}d$ phases formed **A10/14** and **A10/16** are more stable compared to those formed by **B*n*** derivatives, where no crystallization is detected down to room temperature for **A6/14** and **A10/16**, making them good candidates for applications.

4. Summary and conclusions

In summary, we reported the design, synthesis, and molecular self-assembly of the first example of photo switchable HS polycatenars derived form 4-cyanoesorcinol central core unit connected to one short azobenzene-based side arm and a long ester-based wing (**A*n*/6** and **A*n*/10**). The two series differ from each other in the length of the terminal chains at position 3 and 5 in the terminal benezene ring of the long arm. For the shortest homologues of both series (**A6/6** and **A10/6**) non-tilted SmA and tilted SmC phases were observed. The type of tilt in the SmC phases changes from anticlinic (SmC_a) in **A6/6** to synclinic (SmC_s) in **A10/6** with chain elongation. In electro optical investigations of both phases no current peak could be detected, indicating the non-polar nature of these two phases. This behaviour is explained based on the experimental results of the XRD investigations, which confirms an antiparallel side-by-side packing of the molecules in layers with partial interdigitation of the alkyl chains in the aliphatic layers. Such arrangement results in removing the polar order in these smectic phases. On chain elongation in both series the SmC phases are removed and only SmA phases are observed, which once formed on heating do not show any sign of crystallization on cooling down to room temperature in most cases. In addition to SmA phases achiral liquid networks (Iso_1 phases) are detected by DSC investigation. On further chain elongation a transition from the one-dimensional smectic phases to three dimensional achiral bicontinuous cubic phase with $Iadla\bar{3}d$ symmetry ($Cub_{bi}/Ia\bar{3}d$) is observed for the longer homologues of **A10/*n*** series i.e. **A10/14** and **A10/16** as indicated from POM and XRD investigations. These cubic phases are also stable down to ambient temperature, which could be of interest for technological applications. The photoisomerization of the synthesized materials was investigated by UV light irradiation, where a fast and reversible isothermal photo switching between SmC and SmA as well as between SmA and the isotropic liquid phase could be achieved.

CRediT authorship contribution statement

M. Alaasar: Conceptualization, Data curation, Funding acquisition, Investigation, Methodology, Project administration, Supervision, Writing-original draft, Writing-review and editing. **S. Poppe:** Investigation.

Declaration of Competing Interest

The authors declare that they have no known competing financial interests or personal relationships that could have appeared to influence the work reported in this paper.

Acknowledgements

We thank Prof. Dr. Carsten Tschierske for helpful discussion and reading of the manuscript. M. Alaasar acknowledges the German Research Foundation (DFG) for the financial support (AL2378/1-1, 424355983).

Appendix A. Supplementary material

Supplementary data to this article can be found online at https://doi.org/10.1016/j.molliq.2022.118613.

References

[1] T. Kato, J. Uchida, T. Ichikawa, T. Sakamoto, Angew. Chem. Int. Ed. 57 (2018) 4355.
[2] C. Tschierske, Angew. Chem. Int. Ed. 52 (2013) 8828.
[3] C.L. Wang, H.L. Dong, W.P. Hu, Y. Liu, D. Zhu, Chem. Rev. 112 (2012) 2208.
[4] M. Ghedini, D. Pucci, A. Crispini, A. Bellusci, M.L. Deda, I. Aiello, T. Puglieseet, Inorg. Chem. Commun. 10 (2007) 243.
[5] A. Hayer, V. De Halleux, A. Köhler, A. El-Garoughy, E.W. Meijer, J. Barberá, J. Tant, J. Levin, M. Lehmann, J. Gierschner, J. Cornil, Y.H. Geertset, J. Phys. Chem. B. 110 (2006) 7653.
[6] T. Niori, T. Sekine, J. Watanabe, T. Furukawa, H. Takezoe, J. Mater. Chem. 6 (1996) 1231.
[7] R.A. Reddy, C. Tschierske, J. Mater. Chem. 16 (2006) 907.
[8] H. Takezoe, Y. Takanishi, Jpn. J. Appl. Phys. 45 (2006) 597.
[9] A. Eremin, A. Jákli, Soft Matter 9 (2013) 615.
[10] J. Etxebarria, M.B. Ros, J. Mater. Chem. 18 (2008) 2919.
[11] M. Alaasar, Liq. Cryst. 43 (2016) 2208.
[12] T. Sekine, T. Niori, J. Watanabe, T. Furukawa, S.W. Choi, H. Takezoe, J. Mater. Chem. 8 (1997) 1309.
[13] L.E. Hough, M. Spannuth, M. Nakata, D.A. Coleman, C.D. Jones, G. Dantlgraber, C. Tschierske, J. Watanabe, E. Körblova, D.M. Walba, J.E. Maclennan, M.A. Glaser, N.A. Clark, Science 325 (2009) 452.
[14] M. Nagaraj, Liq. Cryst. 43 (2016) 2244.
[15] M. Alaasar, M. Prehm, C. Tschierske, Chem. Eur. J. 22 (2016) 6583.
[16] G. Shanker, M. Nagaraj, A. Kocot, J.K. Vij, M. Prehm, C. Tschierske, Adv. Funct. Mater. 22 (2012) 1671.
[17] O. Francescangeli, V. Stanic, S.I. Torgova, A. Strigazzi, N. Scaramuzza, C. Ferrero, I.P. Dolbnya, T.M. Weiss, R. Berardi, L. Muccioli, S. Orlandi, C. Zannoni, Adv. Funct. Mater. 19 (2009) 2592.
[18] C. Tschierske, D.J. Photinos, J. Mater. Chem. 20 (2010) 4263.
[19] L.A. Madsen, T.J. Dingemans, M. Nakata, E.T. Samulski, Phys. Rev. Lett. 96 (2006).
[20] G.S. Lee, J.S. Cho, J.C. Kim, T.-H. Yoon, S.T. Shin, J. Appl. Phys. 105 (2009).
[21] R. Stannarius, A. Eremin, M.-G. Tamba, G. Pelzl, W. Weissflog, Phys. Rev. E: Stat., Nonlinear, Soft Matter Phys. 76 (2007).
[22] V. Prasad, S.-W. Kang, K.A. Suresh, L. Joshi, Q. Wang, S. Kumar, J. Am. Chem. Soc. 127 (2005) 17224.
[23] D. Jágerová, M. Šmahel, A. Poryvai, J. Macháček, V. Novotná, M. Kohout, Crystals 11 (2021) 1265.
[24] N. Gimeno, I. Pintre, M. Martínez-Abadía, J.L. Serrano, M.B. Ros, RSC Adv. 4 (2014) 19694.
[25] M.V. Srinivasan, P. Kannan, P. Roy, New J. Chem. 37 (2013) 1584.
[26] N.G. Nagaveni, A. Roy, V. Prasad, J. Mater. Chem. 22 (2012) 8948.
[27] N. Trišović, M. Salamonczyk, J. Antanasijević, S. Sprunt, T. Tóth-Katona, A. Jákli, M. Kohout, K. Fodor-Csorba, RSC Adv. 5 (2015) 64886.
[28] M. Horčic, V. Kozmík, J. Svoboda, V. Novotná, D. Pociecha, J. Mater. Chem. C 1 (2013) 7560.
[29] M. Alaasar, M. Prehm, C. Tschierske, RSC Adv. 6 (2016) 82890.
[30] H.K. Bisoyi, Q. Li, Chem. Rev. 116 (2016) 15089.
[31] S.C. Lee, S.H. Lee, O.P. Kwon, J. Mater. Chem. C. 4 (2016) 1935.
[32] T. Ikeda, J. Mamiya, Y.Yu Angew, Chem. Int. Ed. 46 (2007) 506.
[33] E.V. Fleischmann, R. Zentel, Angew. Chem. Int. Ed. 52 (2013) 8810.
[34] M. Kondo, Y. Yu, T. Ikeda, Angew. Chem. Int. Ed. 45 (2006) 1378.
[35] M. Alaasar, M. Prehm, M. Nagaraj, J.K. Vij, C. Tschierske, Adv. Mater. 25 (2013) 2186.
[36] M. Alaasar, M. Prehm, K. May, A. Eremin, C. Tschierske, Adv. Funct. Mater. 24 (2014) 1703.
[37] M. Alaasar, M. Prehm, M.-G. Tamba, N. Sebastian, A. Eremin, C. Tschierske, Chem. Phys. Chem 17 (2016) 278.
[38] M. Alaasar, M. Prehm, S. Belau, N. Sebastián, M. Kurachkina, A. Eremin, C. Chen, F. Liu, C. Tschierske, Chem. Eur. J. 25 (2019) 6362.
[39] I. Wirth, S. Diele, A. Eremin, G. Pelzl, S. Grande, L. Kovalenko, N. Pancenko, W. Weissflog, J. Mater. Chem. 11 (2001) 1642.
[40] L. Kovalenko, M.W. Schröder, R.A. Reddy, S. Diele, G. Pelzl, W. Weissflog, Liq. Cryst. 32 (2005) 857.
[41] C. Keith, A. Lehmann, U. Baumeister, M. Prehm, C. Tschierske, Soft Matter 6 (2010) 1704.

[42] E. Westphal, H. Gallerdo, G.F. Caramori, N. Sebastian, M.-G. Tamba, A. Eremin, S. Kawauchi, M. Prehm, C. Tschierske, Chem. Eur. J. 22 (2016) 8181.
[43] H. Ocak, M. Poppe, B. Bilgin-Eran, G. Karanlık, M. Prehm, C. Tschierske, Soft Matter 12 (2016) 7405.
[44] C. Dressel, T. Reppe, M. Prehm, M. Brautzsch, C. Tschierske, Nat. Chem. 6 (2014) 971.
[45] C. Dressel, F. Liu, M. Prehm, X. Zeng, G. Ungar, C. Tschierske, Angew. Chem. Int. Ed. 53 (2014) 13115.
[46] W. Weissflog, in: J. W. Goodby, J. P. Collings, T. Kato, C. Tschierske, H. F. Gleeson, P. Raynes (Eds.) Handbook of Liquid Crystals, Wiley-VCH, Weinheim, 2nd edn, vol. 5, 2014, pp. 89–174.
[47] L. Han, S. Che, Adv. Mater. 30 (2018) 1705708.
[48] G. Ungar, F. Liu and X. B. Zeng, in: W. Goodby, P. J. Collings, T. Kato, C. Tschierske, H. Gleeson, P. Raynes (Eds.) Handbook of Liquid Crystals, Wiley-VCH, Weinheim, Germany 2014.
[49] N. Marets, D. Kuo, J.R. Torrey, T. Sakamoto, M. Henmi, H. Katayama, T. Kato, Adv. Healthcare Mater. 6 (2017) 1700252.
[50] K. Bisoyi, T.J. Bunning, Q. Li, Adv. Mater. 30 (2018) 1706512.
[51] H.-Y. Hsueh, Y.-C. Ling, H.-F. Wang, L.-Y.C. Chien, Y.-C. Hung, E.L. Thomas, R.-M. Ho, Adv. Mater. 26 (2014) 3225.
[52] R.A. Reddy, U. Baumeister, C. Keith, H. Hahn, H. Lang, C. Tschierske, Soft Matter 3 (2007) 558.
[53] S. Kang, M. Harada, X. Li, M. Tokita, J. Watanabe, Soft Matter 8 (2012) 1916.
[54] J. Matraszek, J. Zapala, J. Mieczkowski, D. Pociecha, E. Gorecka, Chem. Commun. 51 (2015) 5048.
[55] J. Matraszek, D. Pociecha, N. Vaupotič, M. Salamończyk, M. Vogrine, E. Gorecka, Soft Matter 16 (2020) 3882.
[56] M. Alaasar, S. Poppe, Q. Dong, F. Liu, C. Tschierske, Chem. Commun. 52 (2016) 13869.
[57] O. Kwon, X. Cai, W. Qu, F. Liu, J. Szydlowska, E. Gorecka, M.J. Han, D.K. Yoon, S. Poppe, C. Tschierske, Adv. Funct. Mater. 31 (2021) 2102271.
[58] M. Alaasar, A.F. Darweesh, X. Cai, F. Liu, C. Tschierske, Chem. Eur. J. 27 (2021) 14921.
[59] T. Reppe, C. Dressel, S. Poppe, A. Eremin, C. Tschierske, Adv. Optical Mater. 9 (2021) 2001572.
[60] Y. Cao, M. Alaasar, A. Nallapaneni, M. Salamończyk, P. Marinko, E. Gorecka, C. Tschierske, F. Liu, N. Vaupotič, C. Zhu, Phy. Rev. let. 125 (2020).
[61] X. Zeng, G. Ungar, J. Mater. Chem. C. 8 (2020) 5389.
[62] M. Alaasar, M. Prehm, Y. Cao, F. Liu, C. Tschierske, Angew. Chem. Int. Ed. 128 (2016) 320.
[63] M. Alaasar, S. Poppe, Q. Dong, F. Liu, C. Tschierske, Angew. Chem., Int. Ed. 56 (2017) 10801.
[64] M. Alaasar, S. Poppe, Y. Cao, C. Chen, F. Liu, C. Zhu, C. Tschierske, J. Mater. Chem. C (2020) 12902.
[65] G. Pelzl, W. Weissflog, in: A. Ramamoorthy (Ed.) Thermotropic Liquid Crystals: Recent Advances, Springer, Amsterdam, 2007, pp. 1 –58.
[66] D. Pociecha, E. Gorecka, M. Čepič, N. Vaupotič, W. Weissflog, Phys. Rev. E 74 (2006).
[67] A. Eremin, M. Floegel, U. Kornek, S. Stern, R. Stannarius, H. Nadasi, W. Weissflog, C. Zhu, Y. Shen, C.S. Park, J. Maclennan, N. Clark, Phys. Rev. E 86 (2012).
[68] V. Gude, K. Upadhyaya, G. Mohiuddin, V.S.R. Nandiraju, Liq. Cryst. 40 (2013) 120.
[69] F.C. Yu, L.J. Yu, Chem. Mater. 18 (2006) 5410.
[70] S. Kang, Y. Saito, N. Watanabe, M. Tokita, Y. Takanishi, H. Takezoe, J. Watanabe, J. Phys. Chem. B 110 (2006) 5205.
[71] K.M. Fergusson, M. Hird, J. Mater. Chem. 20 (2010) 3069.
[72] A.S. Matharu, C. Grover, L. Komitov, G. Anderson, J. Mater. Chem. 10 (2000), 1303.
[73] W. Weissflog, U. Dunemann, S.F. Tandel, M.G. Tamba, H. Kresse, G. Pelzl, S. Diele, U. Baumeister, A. Eremin, S. Stern, R. Stannarius, Soft Matter 5 (2009) 1840.
[74] M. Monika, V. Prasad, N.G. Nagaveni, Liq. Cryst. 42 (2015) 1490.
[75] R. Deb, R.K. Nath, M.K. Paul, N.V.S. Rao, F. Tuluri, Y. Shen, R. Shao, D. Chen, C. Zhu, I.I. Smalyukh, N.A. Clark, J. Mater. Chem. 20 (2010) 7332.
[76] D.K. Yoon, R. Deb, D. Chen, E. Korblova, R. Shao, K. Ishikawa, N.V.S. Rao, D.M. Walba, I.I. Smalyukh, N.A. Clark, Proc. Nat. Acad. Sci. 107 (2010) 21311.
[77] R.K. Nath, D.D. Sarkar, D.S.S. Rao, N.V.S. Rao, Liq. Cryst. 39 (2012) 889.
[78] M. Alaasar, S. Poppe, C. Tschierske, Liq. Cryst. 44 (2017) 729.
[79] M. Alaasar, S. Poppe, C. Kerzig, C. Klopp, A. Eremin, C. Tschierske, J. Mater. Chem. C 5 (2017) 8454.
[80] M. Alaasar, X. Cai, F. Kraus, M. Giese, F. Liu, C. Tschierske, J. Mol. Liq. (2022), https://doi.org/10.1016/j.molliq.2022.118597, In press.
[81] K. Miyasato, S. Abe, H. Takezoe, A. Fukuda, E. Kuze, Jpn. J. Appl. Phys. 22 (1983) L661.
[82] J.P.F. Lagerwall, F. Giesselmann, Chem. Phys. Chem. 7 (2006) 20.
[83] M. Alaasar, M. Prehm, S. Poppe, C. Tschierske, Chem. Eur. J. 23 (2017) 5541.
[84] E. Enz, S. Findeisen-Tandel, R. Dabrowski, F. Giesselmann, W. Weissflog, U. Baumeister, J. Lagerwall, J. Mater. Chem. 19 (2009) 2950.
[85] M. Alaasar, M. Prehm, Y. Cao, F. Liu, C. Tschierske, Angew. Chem. Int. Ed. 128 (2016) 320.
[86] M. Alaasar, J.-C. Schmidt, X. Cai, F. Liu, C. Tschierske, J. Mol. Liq. 332 (2021).
[87] M. Alaasar, S. Poppe, C. Tschierske, J. Mol. Liq. 277 (2019) 233.
[88] J.M. Shivanna, M. Alaasar, G. Hegde, J. Mol. Liq. 341 (2021).